

## Epidemic analysis of the second-order transition in the Ziff-Gulari-Barshad surface-reaction model

Christopher A. Voigt and Robert M. Ziff

*Department of Chemical Engineering, University of Michigan, Ann Arbor, Michigan 48109-2136*

(Received 22 August 1997)

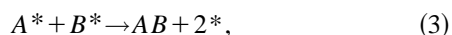
We study the dynamic behavior of the Ziff-Gulari-Barshad irreversible surface-reaction model around its kinetic second-order phase transition, using both epidemic and poisoning-time analyses. We find that the critical point is given by  $p_1 = 0.387\ 368\ 2 \pm 0.000\ 001\ 5$ , which is lower than the previously determined value. We also obtain precise values of the dynamical critical exponents  $z$ ,  $\delta$ , and  $\eta$ , which provide further numerical evidence that this transition is in the same universality class as directed percolation. [S1063-651X(97)51812-5]

PACS number(s): 05.70.Ln, 82.20.Mj, 82.65.Jv

There has been a great deal of interest surrounding the critical behavior of nonequilibrium kinetic models, including directed percolation (DP) [1,2], the contact process [3], and various surface-reaction or catalysis models (for review see [4]). These models all contain a similar continuous (second-order) phase transition from an adsorbing to a vacuum state [5,6].

It has been shown that many of these transitions behave in a universal manner even though the systems abide by different local rules and are inherently modeling different physical systems. Grassberger [1] and Janssen [8] postulated that all single-component continuous transitions fall into the robust DP or Reggeon field theory class, and many numerical simulations have supported this hypothesis (i.e., [6,7,9]). Grinstein, Lai, and Browne [5] were the first to hypothesize that the specific oxygen-poisoning (second-order) transition of the Ziff-Gulari-Barshad (ZGB) surface reaction model [11] falls into this class of models, and Jensen, Fogedby and Dickman ran simulations which support this conclusion [7]. In this communication, we report on new, very extensive simulations that provide further support for this hypothesis, and correct an apparent error in the reported value of the location of that transition. Assuming the identification of the ZGB model with the DP class to be exact, our results give the most accurate values of the DP dynamical critical exponents to date.

The ZGB model is a simplified model for the irreversible reaction of CO ( $A$ ) and  $O_2$  ( $B_2$ ) catalytic reaction on a Pt surface. The simulation involves the adsorption and reaction of species on a square lattice and proceeds via the Langmuir-Hinshelwood mechanism, in which all molecules must adsorb before they can react. The following kinetic scheme is employed:



where  $*$  refers to a lattice site. A Monte Carlo algorithm is employed where a site is randomly chosen. If the site is empty, an  $A$  will adsorb with probability  $p$ . With probability

$1 - p$ , a  $B_2$  is adsorbed and instantly dissociates onto that site and a randomly chosen neighboring site if the latter is empty. When a species adsorbs, it checks for adjacent neighbors of the opposite species. If one is present, the two react immediately, implying an infinite reaction rate as compared to the adsorption rate. There are two transition points in this system. At  $p_2$ , there is a first-order (discontinuous) transition to an  $A$ -poisoned (saturated) state, and at  $p_1$  there is a second-order (continuous) transition to a  $B$ -poisoned state. Between these points exists a reactive window where the system can reach a steady state and react indefinitely. (For a phase diagram, see [11].) Even within the window, for finite systems, the system is only metastable as it can, in principle, poison by a statistical fluctuation to a nonreactive state. However, here the average time to poison  $t_p$  grows exponentially with lattice size  $L$ , the signature of a reactive steady state [12]. The value of  $p_2$  has been accurately determined to be  $0.525\ 60 \pm 0.000\ 01$  [10] using the constant-coverage ensemble algorithm. This algorithm, however, is only applicable to finding the location of the first-order transition.

Because the second-order transition is a continuous one to a single adsorbing state, it is expected to fall into the DP class [6]. Indeed, while the ZGB model involves three components ( $A$ ,  $B$ , and vacant sites), at the second-order transition, there are rarely  $A$  molecules at the surface, so it is essentially a two-species model like other members of the DP class. The value of its transition point  $p_1$  was first empirically observed to be  $0.389 \pm 0.005$  [11]. A more precise value  $0.390\ 65 \pm 0.000\ 10$  was obtained by Jensen, Fogedby, and Dickman using an epidemic analysis [7]. However, while recently performing some other investigations [13], we found that this value appears to be somewhat high. Thus, we carried out new simulations, using the epidemic procedure as well as a poisoning-time analysis, to reexamine the value of  $p_1$  and the related dynamic critical exponents.

The epidemic method was initially used to study the contact process [3] and has been successfully applied to determine the critical exponents and the critical point for DP [1]. To run the epidemic analysis, we started with a large ( $1024 \times 1024$ ) system completely saturated with  $B$  except for a single vacant site in the center. A large system is necessary so that the reactive region never hits the boundary. The simu-

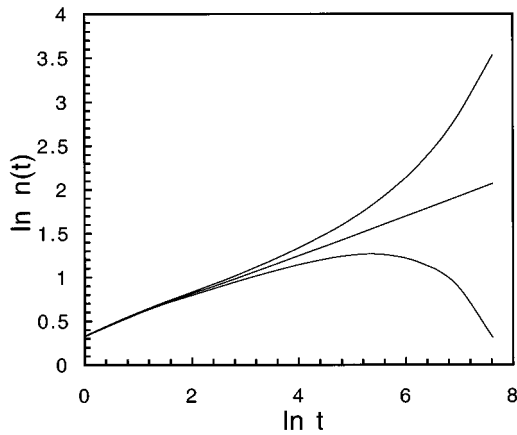


FIG. 1. The behavior of the number of vacant sites  $n$  as plotted against time  $t$ , for  $p=0.390\ 65$ ,  $0.387\ 368\ 2$ , and  $0.384\ 07$  (top to bottom). The upper value is  $p_1$  from [7], and the center is for the value found here.

lation was run at a set value of  $p$  and a reactive cluster was grown and watched until the system reverted to a nonreactive adsorbate state, or a maximum cutoff time was reached.

The vacant sites (numbering  $n_v$ ) were kept on a list that was randomly accessed for each adsorption trial, incrementing the time  $t$  by  $1/n_v$ . As each cluster grew, the quantities of interest were recorded in  $\log_2$  bins of time. Since only approximately 3% of all clusters grown reached the last bin, it was necessary to make numerous runs order to obtain satisfactory statistics. For the values  $p=0.387\ 36$  and  $0.387\ 37$ ,  $8 \times 10^7$  clusters ( $N$ ) were grown up to  $2^{13}=8192$  time steps, requiring a total of 200 days of computational time on a HP 9000 series UNIX platform. In the work of [7] in contrast, only 100 000 to 250 000 clusters were grown up to 1000 time steps. Although we could pinpoint  $p_1$  to four significant figures in just a few hours, we decided to carry out extensive runs in order to find  $p_1$  to six significant digits and to determine the dynamical critical exponents precisely.

We measured the three quantities introduced by Grassberger and de la Torre [3]: the survival probability  $P(t)$ , the mean number of vacancies (averaged over  $N$ )  $n(t)$ , and the mean-square radius of gyration of vacant sites (averaged over  $N$  alive at  $t$ ),  $R^2(t)$ . At the critical point, these are hypothesized to follow the asymptotic power laws,

$$P(t) \sim t^{-\delta}, \quad (4)$$

$$n(t) \sim t^\eta, \quad (5)$$

$$R^2(t) \sim t^z. \quad (6)$$

These exponents follow the hyperscaling relation [3],

$$dz = 2\eta + 4\delta, \quad (7)$$

where  $d$  is the spatial dimension. These relationships provide a powerful method to determine  $p_1$  by evaluating the effects of slightly noncritical values of  $p$ , in which case the resulting behavior deviates from (4)–(6) for large  $t$ . An example of this is shown in Fig. 1, where  $n(t)$  is plotted for  $p$

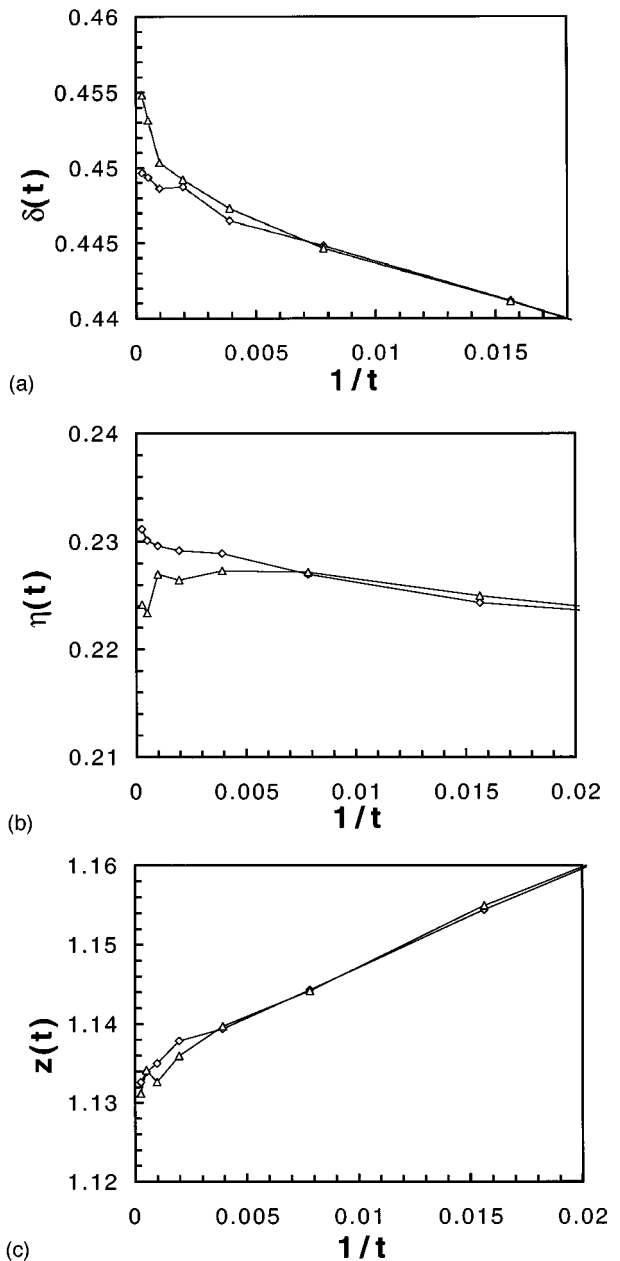


FIG. 2. The three critical exponents derived from our epidemic analysis:  $\delta$  (a),  $\eta$  (b), and  $z$  (c). These values show supercritical ( $\diamond$ :  $p=0.387\ 37$ ) and subcritical ( $\triangle$ :  $p=0.387\ 36$ ) behavior. Each of these lines represents the average of  $3.5 \times 10^7$  runs. The actual value of  $p_1$  falls between these lines and can be determined by linear interpolation as in Fig. 4.

$=0.390\ 65$ ,  $0.387\ 368\ 2$ , and  $0.384\ 07$ . The upper curve is for the value of  $p_1$  reported in [7], while the central curve is for the value we find below.

In order to find the exponents accurately, we consider the local slopes, which are defined as

$$-\delta(t) = \ln[P(t)/P(t/2)]/\ln 2, \quad (8)$$

and similarly for  $\eta(t)$  and  $z(t)$ . (Here we used a factor of 2 rather than 5 or 8 of previous work [2,7], which we could do because of our higher statistics.) These are all graphed in Fig. 2 for  $p=0.387\ 36$  and  $0.387\ 37$ . The local slopes can be

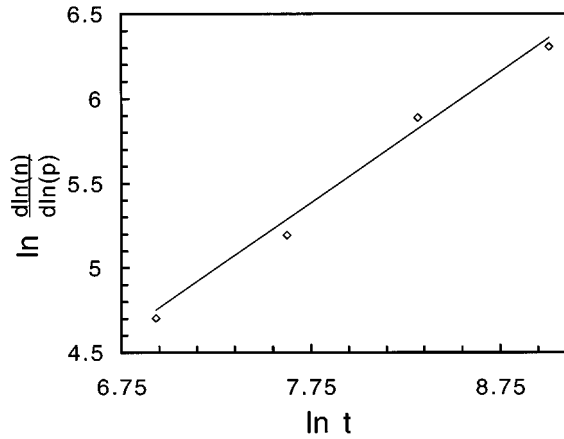


FIG. 3. Plot to determine  $\nu_{\parallel}$  from Eq. (13) by using the values of  $p = 0.387\ 36$  and  $0.387\ 37$ . The line is for  $\nu_{\parallel} = 1.295$  as determined by Grassberger for DP. It can be seen that the ZGB data are consistent with this value.

expanded as [3]

$$\delta(t) = \delta + \frac{a}{t} + \frac{b}{t^{\delta'}}. \quad (9)$$

If the nonanalytic corrections were negligible, then it would be easy to extrapolate the critical exponents as a function of  $1/t$  as discussed by Grassberger. However, these corrections are rather large and, therefore, hinder a direct linear extrapolation. In order to overcome this problem, we grew over  $5 \times 10^8$  clusters to  $2^9$  time steps so that we could better follow the nonanalytical trajectory of each curve. Extrapolating these results to  $t \rightarrow \infty$ , we find

$$\delta = 0.4505 \pm 0.001, \quad \eta = 0.2295 \pm 0.001, \quad z = 1.1325 \pm 0.001, \quad (10)$$

consistent with  $\delta = 0.452 \pm 0.008$ ,  $\eta = 0.224 \pm 0.010$ , and  $z = 1.133 \pm 0.002$  found in [7].

For comparison, the updated values recently found by Grassberger and Zhang [2] for DP are

$$\delta = 0.451 \pm 0.003, \quad \eta = 0.229 \pm 0.003, \quad z = 1.133 \pm 0.002. \quad (11)$$

The precise agreement between Eqs. (10) and (11) leaves little doubt that the ZGB model is included in the DP class as predicted by Grinstein *et al.* [5].

For  $p$  away from  $p_1$ ,  $n(t)$  follows the scaling behavior [3]

$$n(t) \sim t^{-\eta} \phi[(p - p_1)t^{1/\nu_{\parallel}}], \quad (12)$$

and similarly for  $P(t)$  and  $R^2(t)$ . It follows from this equation that

$$\left. \frac{d \ln n}{d \ln p} \right|_{p=p_1} \propto t^{1/\nu_{\parallel}}, \quad (13)$$

where  $\nu_{\parallel}$  is the time-domain correlation length exponent. In Fig. 3, we plot the quantity on the left-hand side of the equation above, calculated by taking the difference of  $n(t)$  for

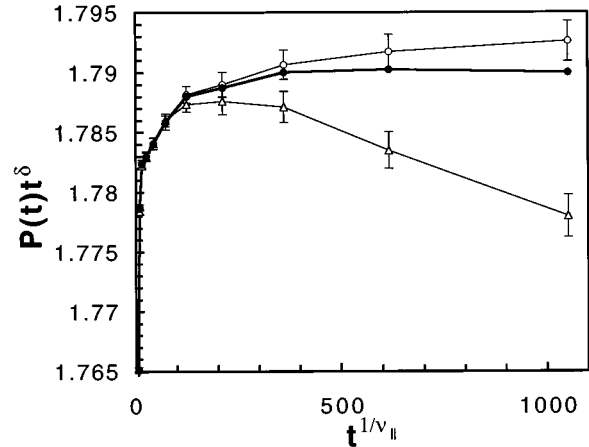


FIG. 4. Plot allowing a linear interpolation for  $p_1$  as expressed in Eq. (14). The lines for  $0.387\ 36$  ( $\Delta$ ) and  $0.387\ 37$  ( $\circ$ ) represent the subcritical and supercritical behavior, respectively. The bold line represents the interpolation for the value,  $p_1 = 0.387\ 368\ 2$ . The error bars were calculated as in Eq. (16). Here,  $t$  is offset by an additive constant 1.7 to improve small-time behavior.

$p = 0.387\ 36$  and  $0.387\ 37$ , vs.  $\ln t$ . This plot shows that Grassberger's value for DP  $\nu_{\parallel} = 1.295 \pm 0.006$  [2] is completely consistent with our data.

To determine the precise value of  $p_1$ , we expand the scaling function  $\phi$  as

$$P(t) \approx t^{-\delta} [a + b(p - p_1)t^{1/\nu_{\parallel}} + \dots]. \quad (14)$$

This equation implies that a plot of  $P(t)t^{\delta}$  vs.  $t^{1/\nu_{\parallel}}$  for values  $p$  close to  $p_1$  should yield straight lines and that a direct linear interpolation of the data from different values of  $p$  can be used to find  $p_1$  (which corresponds to a horizontal line in this plot) (Fig. 4). There is an initial curvature that is to be expected for small clusters due to finite-cluster effects. To minimize this effect, we have added a constant  $c$  to the time that effectively allows for a higher-order analytic correction term:

$$(t + c)^{-\delta} \approx t^{-\delta} \left( 1 - \frac{\delta c}{t} \right), \quad (15)$$

where  $c \approx 1.7$  was found to give the best results. The resulting plot of our data is shown in Fig. 4. The statistical fluctuations in each bin are given by

$$\sqrt{\frac{N_{\text{bin}}(N_{\text{total}} - N_{\text{bin}})}{N_{\text{total}}}}, \quad (16)$$

which implies that the largest bins that have the most accurate data also have the greatest error (least precision). Interpolating the two data curves in Fig. 4, we deduce that  $p_1$  is given by

$$p_1 = 0.387\ 368\ 2 \pm 0.000\ 001\ 5. \quad (17)$$

This result is nearly two orders of magnitude more precise than the result of [7],  $0.390\ 65 \pm 0.000\ 10$ , and more than 30 combined error bars lower. We believe that some error must have occurred in the simulations or analysis of [7,15].

To confirm our value for  $p_1$ , we also ran a poisoning-time analysis [13] of the system at its critical point. Similar methods have been applied to other problems including the quantification of finite lattice effects [12,8,14]. To do this, we essentially run the opposite dynamic algorithm performed by the epidemic analysis. We start with a small lattice in a fully reactive state (all vacant sites) and set the value of  $p$  at our determined  $p_1$ . Periodic boundary conditions are applied and the system is allowed to run until the adsorbate  $B$  saturates or poisons the system, causing a global nonreactive state. When the value of  $p$  is at  $p_1$ , it is expected that the dependence of  $t_p$  on  $L$  will be power-law, and when  $p \neq p_1$ , the dependence will be exponential [12,14]. We ran this simulation for square lattices of powers of 2 in sizes from  $8 \times 8$  to  $64 \times 64$  for roughly  $10^5$  runs each. Here, a time step is defined as  $L^2$  adsorption trials. Figure 5 shows the results of our analysis and it was found that at  $p_1$ , the relationship is indeed

$$t_p \sim L^w \quad (18)$$

with  $w = 1.77 \pm 0.02$ . In [13], we observed that  $w = 2/z = \nu_{\parallel} / \nu_{\perp}$ , indicating that the time to expand a reactive state scales as the time to contract. The  $z$  implied by this result is consistent with the value determined above. While this method is evidently less efficient than the epidemic analysis, it provides a useful confirmation our results for  $p_1$  and  $z$ .

In conclusion, we have provided improved numerical evidence that the ZGB oxygen-poisoning transition falls into the

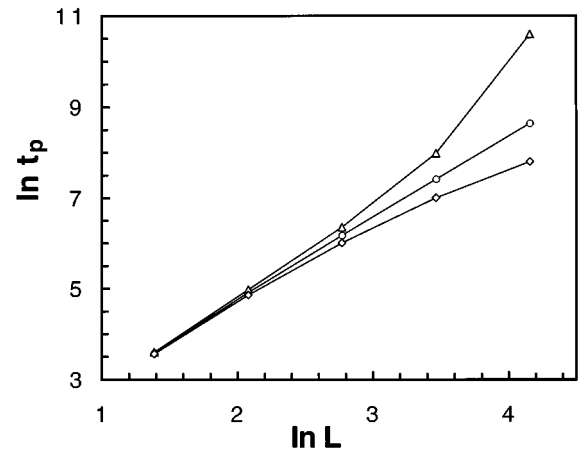


FIG. 5. Results of our poisoning-time analysis for the same values of  $p$  displayed in Fig. 1 ( $\Delta$ , 0.390 65;  $\circ$ , 0.387 368 2;  $\diamond$ , 0.384 07). This plot demonstrates that the expected power-law behavior obtains when our value of  $p_1$  is used.

larger DP class of nonequilibrium models. Accepting that that hypothesis is true, which seems certain, our exponents represent the most accurate values of the DP dynamic critical exponents to date (by a factor of about 2). We also independently confirm that the value of  $\nu_{\parallel}$  for the ZGB model falls into the DP class and use it to find a highly accurate and corrected value of  $p_1$ .

This material is based upon work supported by the U.S. National Science Foundation Grant No. DMR-9520700.

- 
- [1] P. Grassberger, J. Phys. A **22**, 3673 (1989).
  - [2] P. Grassberger and Y. Zhang, Physica A **224**, 169 (1996).
  - [3] P. Grassberger and A. de la Torre, Ann. Phys. (N.Y.) **122**, 373 (1979).
  - [4] E. V. Albano, Heterog. Chem. Rev. **3**, 389 (1997).
  - [5] G. Grinstein, Z. W. Lai, and D. A. Browne, Phys. Rev. A **40**, 4820 (1989).
  - [6] P. Grassberger, Z. Phys. B **47**, 365 (1982).
  - [7] I. Jensen, H. Fogedby, and R. Dickman, Phys. Rev. A **41**, 3411 (1990).
  - [8] H. K. Janssen, Z. Phys. B **42**, 151 (1981).
  - [9] P. Meakin and D. Scalapino, J. Chem. Phys. **86**, 731 (1987).
  - [10] R. M. Ziff and B. Brosilow, Phys. Rev. A **46**, 4630 (1992).
  - [11] R. M. Ziff, E. Gulari, and Y. Barshad, Phys. Rev. Lett. **56**, 2553 (1986).
  - [12] D. ben-Avraham, S. Redner, D. B. Considine, and P. Meakin, J. Phys. A **23**, L613 (1990).
  - [13] C. A. Voigt and R. M. Ziff (to be published).
  - [14] R. Dickman and A. Moreira, xxx.lanl.gov/archive/cond-mat/9709082 (unpublished).
  - [15] The authors of Ref. [7] believe the most likely source of error in their work was a poor quality random number generator. I. Jensen (private communication).